Spectroscopy and Structures of Copper Complexes with Ethylenediamine and Methyl-Substituted Derivatives

Xu Wang and Dong-Sheng Yang*

Department of Chemistry, University of Kentucky, Lexington, Kentucky 40506-0055

Received: March 2, 2006; In Final Form: April 27, 2006

Copper complexes of ethylenediamine (en), *N*-methylethylenediamine (meen), *N*,*N*-dimethylethylenediamine (dmen), *N*,*N*,*N*′-trimethylethylenediamine (tren), and *N*,*N*,*N*′,*N*′-tetramethylethylenediamine (tmen) are synthesized in laser-vaporization supersonic molecular beams and studied by pulsed-field ionization zero electron kinetic energy (ZEKE) and photoionization efficiency spectroscopies and second-order Moller−Plesset perturbation theory. Precise ionization energies and vibrational frequencies of Cu−en, −meen, and −dmen are measured from the ZEKE spectra, and ionization thresholds of Cu−tren and −tmen are estimated from the photoionization efficiency spectra. The measured vibrational modes span a frequency range of 35−1646 cm^{-1} and include metal−ligand stretch and bend, hydrogen-bond stretch, and ligand-based torsion. A number of low-energy structures with Cu binding to one or two nitrogen atoms are predicted for each complex by the ab initio calculations. The combination of the spectroscopic measurements and ab initio calculations has identified a hydrogen-bond-stabilized monodentate structure for the Cu−en complex and bidentate cyclic structures for the methyl-substituted derivatives. The change of the Cu binding from the monodentate to the bidentate mode arises from the competition between copper coordination and hydrogen bonding.

1. Introduction

Ethylenediamine (en) is one of the most widely used nitrogen-containing ligands in coordination chemistry.[1,2] The ligand can adopt staggered trans and gauche conformations about the C−C bond. It is all trans in the solid state[3−5] and largely gauche in the liquid.[6] In the vapor phase, ten rotational isomers have been predicted,[6−12] and the most stable ones are two gauche forms, each with an internal NH···N hydrogen bond.[9] The two gauche forms have a tendency to convert to the trans form when the temperature is increased[9] or the molecules are heated by the absorption of infrared radiation.[12]

In the condensed phases, en complexes of metal ions are mainly in the chelating mode, although examples have been found in monodentate and bridging forms.[2] In the gas phase, experimental and theoretical studies have shown similar bidentate binding modes for a number of metal atoms and ions. Recently, Li et al. studied group 13 (Al, Ga, and In) metal−en complexes by using pulsed-field ionization zero electron kinetic energy (ZEKE) spectroscopy and density functional theory (DFT).[13] Four structural isomers with metal binding to gauche and trans forms of en were predicted by the DFT calculations, and a five-membered cyclic structure was identified by ZEKE spectroscopy. This structure is formed by metal binding to two nitrogen atoms of a gauche en molecule. The bidentate binding mode was also found for Li^+− and Na^+−en by the Hartree−Fock (HF) calculations of Ikuta,[14,15] K/K^+−en by the photoionization efficiency (PIE) measurements and HF/second-order Moller−Plesset perturbation (MP2) calculations of Liau and Su,[16] and Mg^+−en by the photoframentation experiments and DFT calculations of Liu et al.[17] Above the bidentate structure, these calculations located a monodentate form of Li^+/Na^+−en with the metal ions binding to single nitrogen of trans en,[14,15] a hydrogen-bonded monodentate form of Mg^+−en with Mg^+ binding to a nitrogen atom of gauche en,[17] and three monodentate forms of K^+/K−en with or without internal hydrogen bonding.[16] More closely related to this work was a DFT study of the potential energy surface associated with the gas-phase reactions between en and Cu^+ by Alcami et al.[18,19] From the DFT calculation, the most stable association complex of Cu^+−en was a bidentate cyclic structure, a second minimum was a hydrogen-bond stabilized monodentate structure, and two other local minima were found with Cu^+ binding to the trans isomer of en.

In this paper, we report the ZEKE study of the Cu complexes with en, *N*-methylethylenediamine (meen), *N*,*N*-dimethylethylenediamine (dmen), *N*,*N*,*N*′-trimethylethylenediamine (tren), and *N*,*N*,*N*′,*N*′-tetramethylethylenediamine (tmen). The ZEKE spectra of Cu−en, −meen, and −dmen are analyzed by using MP2 and Franck−Condon (FC) calculations. In contrast to the previously reported metal−en complexes, the neutral Cu−en complex prefers a monodentate binding mode, where Cu binds to a nitrogen atom of a hydrogen-bonded gauche en molecule. More interestingly, methyl substitutions of one or more hydrogen atoms of the NH_2 groups switches the Cu binding from the monodentate to bidentate mode.

2. Experimental and Computational Methods

Experimental measurements were performed with our home-built metal cluster beam ZEKE spectrometer.[20] Metal complexes were prepared by reactions of copper atoms with the vapor of a diamine ligand [$NH_2CH_2CH_2NH_2$, 99.5%, Aldrich; $CH_3NHCH_2CH_2NH_2$, 95%, TCI; $(CH_3)_2NCH_2CH_2NH_2$, 99%, Aldrich; $(CH_3)_2NCH_2CH_2NHCH_3$, 96%, TCI; $(CH_3)_2NCH_2CH_2N(CH_3)_2$, 99%, Aldrich] in molecular beams. Copper atoms were

* dyang0@uky.edu.

10.1021/jp061325q CCC: $33.50
Published on Web 05/25/2006

produced by pulsed laser vaporization of a copper rod (99.9%; Alfa Aesar) with the second harmonic output of a Nd:YAG (neodymium: yttrium aluminum garnet) laser (Quanta-Ray, GCR-3, 532 nm, ~3 mJ) in the presence of a carrier gas (He or Ar, UHP, Scott-Gross) of ~50 psi. The carrier gas was delivered by a piezoelectric pulsed valve.[21] The metal rod was translated and rotated by a motor-driven mechanism to ensure that each laser pulse ablate a fresh metal surface. The vapor of the diamine ligand was introduced at room temperature and through a stainless capillary to a small reaction chamber (~1.5 mL). This chamber was located downstream of the ablation region, where the ligand interacted with the copper atoms entrained in the carrier gas.

Molecular species in the supersonic beam were identified by time-of-flight mass spectrometry. The ultraviolet photon source used for ionization was a frequency-doubled dye laser (Lumonics, HD-500), pumped by a XeCl excimer laser (Lumonics, PM-800). Ion signals of 1:1 metal−ligand complexes were optimized by adjusting the timing and power of the ablation and photoionization lasers, the vapor pressure of the ligand, and the backing pressure of the carrier gas. Prior to ZEKE experiments, ionization thresholds of the 1:1 complexes were located by recording the ion signal as a function of laser wavelength. ZEKE electrons were produced by photoexcitation of neutral molecules to high-lying Rydberg states, followed by ~3 μs delayed pulsed electric field ionization (1.2 V cm^{-1}, 100 ns) of these Rydberg states. A small dc field of ~0.08 V cm^{-1} was applied to help separate ZEKE electrons from kinetic electrons produced by direct photoionization. The pulsed electric field was generated by a digital delay-pulse generator (SRS, DG535). The ion and electron signals were detected by a dual microchannel plate detector (Galileo), amplified by a preamplifier (SRS, SR445), averaged by a gated integrator (SRS, SR250), and stored in a laboratory computer. Laser wavelengths were calibrated against vanadium or titanium atomic transitions.[22] Field-dependent measurements were not carried out because of the limited size of the ZEKE signal.

Geometry and frequency calculations were carried out with the MP2 method and 6-311+G(d,p) basis, implemented in the *Gaussian 03* program package.[23] Multidimensional FC factors were calculated from the equilibrium geometries, harmonic frequencies, and normal coordinates.[24,25] In these FC factor calculations, the Duschinsky effect[26] was considered to account for normal mode differences between the neutral molecule and ion. Spectral broadening was simulated by giving each line a Lorenztian line shape with the line width of the experimental spectrum. Transitions from excited vibrational levels of the neutral electronic states were considered by assuming thermal excitations at specific temperatures.

3. Results and Discussion

3.1. Computation. *3.1.1. Isomers of Free Ligands.* To determine the structures of the metal complexes, we first consider the low-energy conformers of the free ligands. Although a large number of rotational isomers have been predicted for en, only three were identified by electron diffraction[9] or infrared spectroscopic measurements.[12] Figure 1 displays the most stable gauche (A,B) and trans isomers of en, and Table 1 lists their geometries and relative energies from the MP2/6-311+G(d,p) calculations. Both gauche isomers are more stable than the trans form, due to the stabilization of the internal NH···N hydrogen bonding. This prediction is consistent with the previous MP2 [6,10] and B3LYP[13] calculations. Gauche A has a shorter NH···N distance, a larger ∠N−C−C−N dihedral angle,

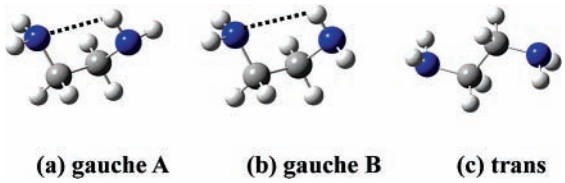

Figure 1. Low-energy rotational isomers of ethylenediamine.

and a slightly lower energy than gauche B, while both gauche forms have the same ∠H−N···H angles. The two gauche forms are different because of the different orientations of the proton donor NH_2 group. To estimate the hydrogen-bond strength, we calculated a gauche conformer in C_2 symmetry with a twofold axis passing through the middle point of the C−C bond. This structure has a hydrogen−nitrogen distance of 2.83 Å, which is larger than the sum of the van der Waals radii of nitrogen (1.55 Å) and hydrogen (1.20 Å).[27] By neglecting the hydrogen-bonding interaction in this C_2 structure, we estimated the hydrogen-bond dissociation energy of 17.8 kJ mol^{-1} for the most stable gauche form. This value is larger than the dissociation energy of 12.2 kJ mol^{-1} for ammonia dimer.[28]

The relative stability of the three isomers of meen and dmen follow the same order as that of the parent diamine (Table 1), and the energy differences between the gauche (A,B) and trans forms increase with increasing number of methyl groups. The N−C−C−N framework remains planar in the trans dmen, but it is nonplanar in the trans meen because of the asymmetric $NHCH_3$ group. For the gauche isomers, the ∠N−C−C−N dihedral angle slightly decreases from en through meen to dmen, while the N···H bond distance and ∠N−H···N angle show no significant changes. The calculations of the hydrogen-bond energies of meen and dmen are not straightforward, because the energies of the non-hydrogen-bonded configurations depend on the relative orientation of the methyl groups. However, a Mulliken population analysis of gauche A shows the negative charges on the nitrogen atom of the proton acceptor NH_2 [$NHCH_3$ or $N(CH_3)_2$] decreases from en (−0.43) to meen (−0.33) to dmen (−0.08). Since the positive charges on the hydrogen atoms of the proton donor NH_2 groups are almost the same (~0.25) in the three amines, the decrease of the negative charges on the nitrogen atom should reduce the Coulomb attraction between the hydrogen and nitrogen atoms. This agrees with the previous predictions that methyl substitutions deplete the charges of the proton acceptors of nitrogen bases [29−31] and reduce the strengths of the internal hydrogen bonding of nitrogen- and oxygen-containing dimers.[32−34]

The trimethyl-substituted diamine ligand has only one hydrogen atom available to form a NH···N hydrogen bond in the gauche A form. In comparison to dmen, the gauche A isomer of tren has a significantly longer NH···N distance and smaller −N−H···N angle (Table 1), indicating a weaker hydrogen bond in this trimethyl-substituted derivative. The weakening of the hydrogen bond in tren is due to the reduced electrostatic interaction and the increased steric hindrance. The reduced electrostatic attraction arises from the decrease of the positive charge on the hydrogen atom of the proton donor upon the additional methyl substitution. For the gauche B isomer, a CH···N hydrogen bond is predicted, where the CH_3 group acts as the proton donor (Figure 2a). A CH···N hydrogen bond is normally considered to be weak, because the carbon atom is not very electronegative. However, this type of the hydrogen bond has been identified in a variety of organic and organometallic compounds.[35−38] Interestingly, the CH···N bond of the gauche B isomer has a shorter H···N distance and a larger ∠C−H···N angle than the NH···N bond of gauche A (Table 1),

TABLE 1: Relative Electronic Energies (E_e, kJ mol^{-1}) and Geometries (R, Å; ∠, deg) of Ethylenediamine and Methyl-Substituted Derivatives from MP2/6-311+G(d,p) Calculations

molecules	conformers[a]	E_e	R(H···N)	∠N−H···N	∠N−C−C−N
$H_2N(CH_2)_2NH_2$, en	gauche A	0	2.450	105.0	63.9
	gauche B	1.6	2.533	105.0	60.2
	trans	8.2			180.0
$(CH_3)HN(CH_2)_2NH_2$, meen	gauche A	0	2.440	105.7	61.8
	gauche B	1.6	2.534	105.3	58.2
	trans	11.1			177.4
$(CH_3)_2N(CH_2)_2NH_2$, dmen	gauche A	0	2.446	105.7	60.3
	gauche B	1.9	2.549	105.3	56.9
	trans	15.2			180.0
$(CH_3)_2N(CH_2)_2NH(CH_3)$, tren	gauche A	0	2.595	100.3	51.4
	gauche B	6.5	2.489	120.2[b]	66.5
	trans	18.0			176.8
$(CH_3)_2N(CH_2)_2N(CH_3)_2$, tmen	gauche	0	2.367	126.0[b]	70.2
	trans	15.7			180.0

[a] All conformers are in the C_1 point group except for the trans conformers of en (C_{2h}), dmen (C_s), and tmen (C_{2h}). All gauche conformers have a NH···N hydrogen bond, except for the gauche B of tren and the gauche form of tmen, both of which have a CH···N hydrogen bond. [b] −C−H···N.

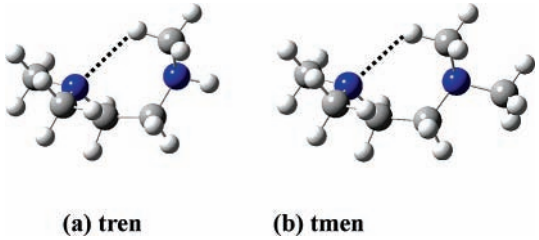

Figure 2. CH···N hydrogen-bonded isomers of trimethylethylenediamine (a) and tetramethylethylenediamine (b).

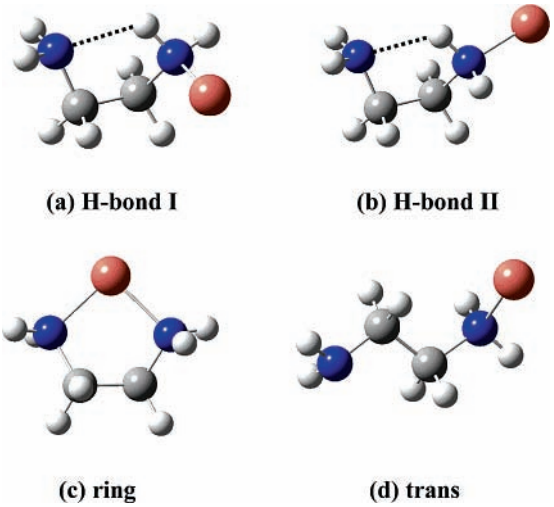

Figure 3. Rotational isomers of Cu−ethylenediamine.

although the hydrogen atom in CH···N is less positively charged than that in NH···N.

The formation of the NH···N hydrogen bond is not possible in the tetramethyl-substituted diamine, because all four hydrogen atoms in the two NH_2 groups are replaced by methyl groups. Thus, only a gauche isomer containing a CH···N bond is predicted for this molecule (Figure 2b). The gauche tmen shows a shorter CH···N distance and larger ∠C−H···N and ∠N−C−C−N angles than the gauche B tren. The larger angles are due to the increased steric effect in the tetramethyl-substituted diamine.

3.1.2. Isomers of Cu−en. Figure 3 displays the H-bond I, H-bond II, ring, and trans isomers of Cu−en, with their geometries and relative energies listed in Table 2. The H-bond I and II isomers are formed by Cu binding with single nitrogen of gauche A and B. They have the same Cu−N distances and nearly identical hydrogen-bond lengths. H-bond I is slightly more stable than H-bond II. The major difference between the two hydrogen-bonded monodentate isomers is the ∠Cu−N−C−C dihedral angle, which is 72.0° in H-bond I and 169.7° in H-bond II. The differential dihedral angles are due to the different orientations of the proton donor NH_2 groups of the gauche A and B forms. Upon Cu coordination, the hydrogen-bond distances are reduced, and the ∠N−H···N angles are increased. The negative charge of the nitrogen atom of the proton acceptor is increased from (−0.43) in the free gauche A form to (−0.53) in the complex, and the positive charge of the hydrogen atom of the proton donor is increased from 0.27 to 0.30. These changes in the hydrogen-bond geometry and atomic charge suggest that Cu coordination enhances the hydrogen bonding. The ring structure is formed by Cu binding to both nitrogen atoms of the gauche A or B forms and has a twofold axis passing through the Cu atom and the middle point of the C−C bond. This bidentate cyclic structure has a slightly higher energy than the monodentate H-bond I complex but a significant lower ionization energy. The bidentate structure also has a longer Cu−N distance than the monodentate complex, as expected by considering coordination numbers. The fourth conformer of the Cu−en complex is formed by Cu binding to single nitrogen atom of the trans ligand and has the highest energy among all the isomers. The different stabilities between the monodentate trans and hydrogen-bonded structures are clearly due to the effect of the internal hydrogen bonding.

It is interesting to compare the binding modes of Cu−en with other metal−en complexes, for which structures have been determined.[13] The hydrogen-bond-stabilized monodentate structures of the neutral Cu−en complex are more stable than the bidentate cyclic structure, whereas the most stable structure of the group 13 metal−en complexes is in the bidentate binding mode. Although the en ligand has two nitrogen binding sites, the actual binding mode depends on the competition between the hydrogen bonding and metal coordination. The group 13 metal atoms have an unpaired np electron, and the p orbital can orientate itself perpendicularly to the nitrogen lone-pair electron orbital to minimize the electron repulsion. On the other hand, the Cu $4s^1$ electron has a high density along the nitrogen lone-pair orbital, which causes strong electron repulsion. As a result, the group 13 metal atoms bind N atom more strongly than Cu atom. For example, the metal−ligand bond dissociation energy of the bidentate Al−en complex is calculated to be 78.4 kJ mol^{-1}, while that of the bidentate Cu−en is 50.0 kJ mol^{-1}.

TABLE 2: Relative Electronic Energies (E_e, kJ mol^{-1}), Adiabatic Ionization Energies (AIE, eV), Bond Dissociation Energies (D_0, kJ mol^{-1}), and Geometries (R, Å; ∠, deg) of Copper−Diamine Complexes from MP2/6-311+G(d,p) Calculations

complexes[a]	E_e	AIE	D_0	R(Cu−N)	R(N···H)	∠N−Cu−N	∠N−H···N	∠Cu−N−C	∠N−C−C−N
					Cu−en				
H-bond I	0	5.03	53.5	2.02	2.32		109.3	116.0	58.7
H-bond II	2.2	4.99	52.8	2.02	2.39		108.8	116.3	57.3
ring	4.0	4.08	50.0	2.17		81.6		107.4	56.7
trans	14.5	5.19	47.4	2.03				117.2	176.6
					Cu^+−en				
H-bond I	90.6		268.0	1.92	2.13		114.8	118.0	51.4
H-bond II	89.2		270.6	1.91	2.10		117.6	118.6	51.2
ring	0		355.5	2.01		92.6		100.1	58.1
trans	120.9		246.8	1.93				115.2	179.7
					Cu−meen				
H-bond I	2.0	4.98	55.3	2.02	2.36		110.3	116.3	54.8
H-bond II	0	5.01	55.9	2.02	2.31			116.0	57.6
ring	2.2	4.05	54.3	2.19/2.16		82.0		105.6/108.1	57.0
trans-L	17.8	5.21	49.5	2.05				111.4	174.5
trans-S	18.6	5.21	48.7	2.03				115.7	177.8
					Cu^+−meen				
H-bond I	92.7		274.7	1.91	2.07		119.2	118.8	50.0
H-bond II	93.5		272.5	1.91	2.08		117.5	117.9	49.9
ring	0		363.2	2.01		93.6		99.4/100.6	58.6
trans-L	131.1		246.9	1.93				112.1	171.8
trans-S	132.4		245.6	1.92				116.6	179.7
					Cu−dmen				
H-bond I	2.7	4.98	53.4	2.02	2.36		110.8	116.4	53.5
H-bond II	0	5.02	57.4	2.02	2.31		109.7	115.9	56.3
ring	2.4	4.04	54.4	2.23/2.14		82.2		104.2/108.6	56.8
trans-L	23.3	5.20	48.5	2.08				107.3	180
trans-S	22.0	5.19	49.4	2.03				115.7	180
					Cu^+−dmen				
H-bond I	94.6		272.3	1.91	2.04		120.8	118.9	48.7
H-bond II	95.5		272.8	1.91	2.07		118.2	117.7	49.1
ring	0		364.2	2.01/ 2.00		94.6		98.2/100.0	58.5
trans-L	137.1		246.0	1.94				108.1	180.0
trans-S	134.3		248.1	1.92				116.5	180.0
					Cu−tren				
H-bond I	1.3	4.95	57.2	2.03	2.37		109.0	113.2	48.7
H-bond II	10.8		54.0	2.04	2.44		120.3[b]	115.2	61.3
ring	0	4.00	59.2	2.22/2.16		82.7		104.8/106.4	57.6
trans-L	27.2	5.17	49.5	2.07				107.2	177.9
trans-S	25.0	5.15	51.2	2.05				111.3	168.7
					Cu^+−tren				
H-bond I	96.5		279.1	1.91	2.02		122.2	115.1	44.5
ring	0		372.8	2.01/2.00		95.7		97.9/98.5	59.1
trans-L	143.5		250.4	1.94				108.0	173.1
trans-S	138.9		254.1	1.93				112.0	163.5
					Cu−tmen				
H-bond	13.0		53.2	2.06	2.33		125.4[b]	112.9	65.2
ring	0	3.99	66.0	2.20		83.1		105.2	57.1
trans	31.6	5.15	50.0	2.07				107.0	180.0
					Cu^+−tmen				
ring	0		380.5	2.00		96.6		97.4	58.9
trans	146.6		252.7	1.94				107.7	180.0

[a] All complexes are in the C_1 point group, except for the ring structures of Cu/Cu^+−en and −tmen (C_2) and the trans structures of Cu/Cu^+−dmen and −tmen (C_s). All H-bonded complexes have a NH···N hydrogen bond, except for H-bond II Cu−tren and H-bond Cu−tmen, which have a CH···N hydrogen bond. [b] -C−H···N.

Another interesting difference between Cu and group 13 metal atoms concerns their trans structures. The trans structure of Cu−en has a twist NCCN chain, while the group 13 metal−en trans form has C_s symmetry with a planar NCCN framework.[13] The C_s trans structure of Cu−en is not a local minimum.

Ionization removes the Cu 4s-based electron from the highest occupied molecular orbital of the neutral complex. The removal of the Cu 4s electron reduces the electron repulsion with the nitrogen electron lone pair and creates additional electrostatic interaction between Cu^+ and en. As a result, the copper−nitrogen bond distance is reduced, and the metal−ligand bond energy is dramatically enhanced for all four conformers. As metal−ligand bond energy increases, the bidentate cyclic ion becomes more stable than the monodentate hydrogen-bonded ions, consistent with the previous DFT calculations.[18,19] The ratio of the bond energies of the ionized species to the neutral species is about five for the monodentate conformers, whereas this ratio is seven for the bidentate conformer. The larger binding energy of the cyclic structure of the ion leads to the lower ionization energy of the cyclic structure. In addition to the

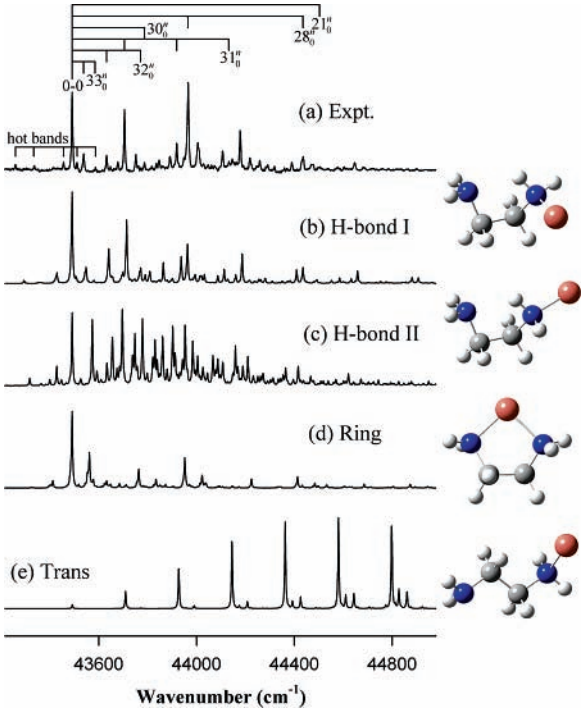

Figure 4. Experimental ZEKE spectrum of Cu−ethylenediamine and simulations of four Cu−ethylenediamine isomers (b−e).

changes in metal−ligand geometry and thermochemistry, ionization causes further changes in the ligand geometry. For example, the hydrogen-bond distances in H-bond I and II are reduced by as much as 10%. Moreover, the negative charge of the hydrogen-bonded nitrogen atom and the positive charge of the hydrogen-bonded hydrogen atom are slightly increased from the neutral complex (−0.53, 0.30) to the ion (−0.57, 0.33), which suggests that the hydrogen bonding may be enhanced upon ionization.

3.1.3. Isomers of Cu−meen, −dmen, −tren, and −tmen. Similar to Cu−en, the copper complexes of the methyl-substituted derivatives possess low-energy structures in the monodentate and bidentate binding modes (Table 2). Both H-bond I and II of Cu−meen and −dmen and H-bond I of Cu−tren contain an internal NH···N hydrogen bond, whereas H-bond II of Cu−tren and the only hydrogen-bonded structure of Cu−tmen have an internal CH···N hydrogen bond. The structures containing the CH···N bond are not stable upon ionization and convert to the bidentate cyclic structures in the ions. Cu−meen and −tren have two trans monodentate structures (trans-L and tran-S), because the monomethyl- and trimethyl-substituted ligands have asymmetric amine groups. All of the methyl-substituted complexes form a bidentate cyclic structure, which becomes more stable with increasing methyl substitutions. As a result, the bidentate structures of the neutral Cu−tren and −tmen complexes have lower energies than the hydrogen-bonded monodentate structures. The increased stability of the bidentate versus hydrogen-bonded structures is due to the weakening of the internal hydrogen bond and the strengthening of the metal coordination with methyl substitutions. Similar methyl effects have been reported for hydroxyl-containing dimers[33] and metal−amine complexes.[39−42]

3.2. Spectroscopy. *3.2.1. ZEKE Spectra of Cu−en.* Figure 4a shows the experimental ZEKE spectrum of Cu−en seeded in an argon carrier gas.[43] The spectrum displays a strong 0−0 transition peak at 43 491(5) cm^{-1} with the full width at half-maximum height (fwhm) of ∼5 cm^{-1}, and vibrational intervals of 1013, 474, 296, 214, 141, and 47 cm^{-1}. Additionally, the

TABLE 3: Adiabatic Ionization Energies (AIE) of Copper−Amine Complexes from ZEKE Spectra

molecules	AIE (cm^{-1})	refs
$Cu-NH_3$	46485 (5)	45
$Cu-NH_2(CH_3)$	45511 (5)	42
$Cu-NH(CH_3)_2$	44916 (5)	42
$Cu-N(CH_3)_3$	44730 (5)	44
$Cu-(NH_3)_2$	29532 (5)	46
$Cu-H_2NCH_2CH_2NH_2$	43491 (5)	this work
$Cu-(CH_3)HNCH_2CH_2NH_2$	36020 (10)	this work
$Cu-(CH_3)_2\ NCH_2CH_2NH_2$	36284 (10)	this work
$Cu-(CH_3)_2\ NCH_2CH_2NH(CH_3)$	36250 (300)[a]	this work
$Cu-(CH_3)_2\ NCH_2CH_2N(CH_3)_2$	34950 (300)[a]	this work

[a] From photoionization efficiency measurements.

spectrum exhibits a number of hot transitions originating from excited vibrational levels of the ground electronic state of the neutral complex. The 0−0 transition energy of Cu−en is comparable to the adiabatic ionization energy (AIE) of simple Cu−amine complexes $Cu-NH_n(CH_3)_{3-n}$ ($n = 0-3$) but much higher than the AIE of $Cu-(NH_3)_2$ (Table 3).[42,44−46] The $Cu-NH_n(CH_3)_{3-n}$ complexes are formed by single copper−nitrogen coordination, whereas $Cu-(NH_3)_2$ is formed by Cu binding to two nitrogen atoms.[46] Thus, the 0−0 transition energy of Cu−en likely corresponds to the AIE from the monodentate neutral complex to the monodentate ion. Among the measured vibrational intervals, the 474 cm^{-1} spacing can be assigned to the Cu^+-N stretch of Cu^+-en, because it is comparable to the Cu^+-N stretching frequencies of Cu^+-NH_3 (470 cm^{-1}),[45] $Cu^+-NH_2CH_3$ (461 cm^{-1}),[42] and $Cu^+-NH(CH_3)_2$ (482 cm^{-1}).[42] Assignments for other transitions are discussed below in combination with spectral simulations.

Figure 4b−e shows the spectral simulations of H-bond I, H-bond II, ring, and trans isomers. These simulations represent the vibronic transitions from the doublet ground electronic state of the neutral molecule to the singlet ground electronic state of the ion. The theoretical 0−0 transition energies are shifted to the experimental value for simplicity, but the calculated vibrational frequencies are not scaled in these simulations. Electronic transitions from one isomer of the neutral complex to another isomer of the ion are not considered, because such transitions would have a long FC profile due to large geometry differences between the initial and final states. The simulation of H-bond I (Figure 4b) is in nice agreement with the measured spectrum, while others are very different. Thus, the observed spectrum is attributed to H-bond I, and no significant contributions are from other isomers. The experimental finding is consistent with the MP2 prediction that the H-bond I isomer has the lowest energy for the neutral complex. Other low-energy isomers might be formed in the molecular beams, but searches of PFI-ZEKE signals around their predicted AIEs were not successful.

The experimental spectrum can be assigned in comparison with the simulation of the H-bond I isomer. Major progressions involving the excitation of single vibrational mode (e.g., 21_0^n, 28_0^n, 30_0^n, 31_0^n, 32_0^n, 33_0^n) are labeled in Figure 4a, more detailed assignments are listed in Table 4, and vibrational frequencies obtained from the spectrum are summarized in Table 5. Six vibrational modes have been measured for the ion and three for the neutral complex. The ion modes include N−C (ν_{21}^+), Cu^+-N (ν_{28}^+), and H-bond stretches (ν_{31}^+), NH_2 rock (ν_{30}^+), Cu^+-N-C bend (ν_{32}^+), and $Cu^+-N-C-C$ torsion (ν_{33}^+). The neutral modes include H-bond stretch (ν_{31}), Cu−N−C bend (ν_{32}), and Cu−N−C−C torsion (ν_{33}). Among these measured vibrational modes, the copper−nitrogen and hydrogen-bond

TABLE 4: ZEKE Peak Wavenumber and Assignment of the Cu−Diamine Complexes

Cu−en				Cu−meen		Cu−dimeen	
positions	assignments	positions	assignments	positions	assignments	positions	assignments
43259	$31_1^0 33_1^0$	44027	$31_0^1 32_0^2 33_0^1$	36022	0_0^0	36284	0_0^0
43336	$32_1^0 33_1^0$	44048	$30_0^1 31_0^1 33_0^1$	36224	40_0^1	36428	50_0^1
43456	33_1^0	44061	$28_0^1 33_0^2/31_0^2 32_0^1$	36426	40_0^2	36483	49_0^1
43491	0_0^0	44073	$31_0^1 32_0^2 33_0^2$	36472	$38_0^1 40_0^1/35_0^1$	36559	$49_0^2 50_1^0$
43511	32_1^1	44107	$28_0^1 32_0^1$	36596	$38_0^1 40_0^2 42_1^0$	36682	49_0^2
43538	33_0^1	44132	31_0^3	36628	40_0^3	36764	$48_0^1 49_0^2 50_1^0$
43587	33_0^2	44146	$30_0^1 31_0^1 32_0^1$	36676	$38_0^1 40_0^2/35_0^1 40_0^1$	36881	49_0^3
43632	32_0^1	44178	$28_0^1 31_0^1$	36796	$38_0^1 40_0^3 42_1^0$	36977	$48_0^2 49_0^2 50_1^0$
43648	32_1^2	44219	$28_0^1 31_0^1 33_0^1$	36830	40_0^4	37025	$49_0^3 50_0^1$
43678	$32_0^1 33_0^1$	44247	$28_0^1 32_0^2$	36875	$38_0^1 40_0^3$/	$35_0^1 40_0^2$37079	49_0^4
43705	31_0^1	44258	$28_0^1 30_0^1$	37031	40_0^5	37151	$41_0^1 49_0^2$
43752	$31_0^1 33_0^1$	44291	$28_0^1 32_0^2 33_0^1$	37079	$38_0^1 40_0^4/35_0^1 40_0^3$	37219	$49_0^4 50_0^1$
43762	$32_0^2 33_1^1$	44319	$28_0^1 31_0^1 32_0^1$	37126	$40_0^5 42_0^1$	37276	49_0^5
43771	32_0^2	44389	$28_0^1 31_0^2$	37231	40_0^6	37347	$41_0^1 49_0^3$
43787	30_0^1	44436	28_0^2	37277	$38_0^1 40_0^5$/	$35_0^1 40_0^4$37418	$49_0^5 50_0^1$
43816	$32_0^2 33_0^1$	44470	$28_0^1 30_0^1 31_0^1$	37326	$40_0^6 42_0^1$	37468	49_0^6
43836	$30_0^1 33_0^1$	44481	$28_0^2 33_0^1$	37432	40_0^7	37548	$41_0^1 49_0^4$
43847	$31_0^1 32_0^1$	44504	21_0^1	37478	$38_0^1 40_0^6/35_0^1 40_0^5$	37596	25_0^1 [a]
43891	$31_0^1 32_0^1 33_0^1$	44575	$28_0^2 32_0^1$			37665	49_0^7
43919	31_0^2	44603	$28_0^1 31_0^3$			37739	$41_0^1 49_0^5$
43965	28_0^1	44647	$28_0^2 31_0^1$			37866	49_0^8
44010	$28_0^1 33_0^1$	44685	$28_0^1 30_0^1 31_0^2$			37941	$41_0^1 49_0^6$
						37999	13_0^1 [a]

[a] Tentative assignments; see the text.

TABLE 5: Adiabatic Ionization Energies (AIE, eV) and Vibrational Frequencies (cm^{-1}) of Cu−Diamine Complexes from ZEKE Measurements and MP2/6-311+G(d,p) Calculations

complexes	vibrational description		ZEKE	MP2
Cu−en		AIE	43491(5)	40600
	N−C stretch	ν_{21}^+	1013	1062
	Cu−N stretch (with N displacement)	ν_{28}^+	474	473
	NH_2 rock	ν_{30}^+	296	318
	H-bond stretch	ν_{31}^+/ν_{31}	214/197	223/197
	Cu−N−C bend	ν_{32}^+/ν_{32}	141/121	150/133
	Cu−N−C−C torsion	ν_{33}^+/ν_{33}	47/35	57/62
Cu−meen		AIE	36022(10)	32665
	Cu−N stretch (with N displacement)	ν_{35}^+	449	471
	NCCNC twist	ν_{38}^+	248	259
	Cu−N stretch (with Cu displacement)	ν_{40}^+	201	213
	NCCNC twist	ν_{42}^+/ν_{42}	95/80	109/79
Cu−dmen		AIE	36284(10)	32590
	NH_2 scissor	ν_{13}^+	1646	1644
	CH_2 rock	ν_{25}^+	1312	1334
	Cu−N stretch (with N displacement)	ν_{41}^+	469	494
	N−Cu−N bend	ν_{48}^+	209	212
	Cu−N stretch (with Cu displacement)	ν_{49}^+	199	207
	$N-(CH_3)_2$ rock	ν_{50}^+/ν_{50}	144/123	160/119
Cu−tren		IE	36250(300)[a]	32260
Cu−tmen		IE	34950(300)[a]	32180

[a] From photoionization efficiency measurements.

vibrations are of the most importance, because they provide direct evidence about the metal−ligand binding and molecular structures. The Cu−N stretching frequency increases from the neutral complex (353 cm^{-1}, MP2) to the ion (474 cm^{-1}), as ionization enhances the metal−ligand binding. It is interesting to note that the monodentate Cu^+−en ion has a very similar Cu^+−N stretching frequency as $[Cu(en)_3]^{2+}SO_4^{2-}$ (485 cm^{-1}) in the condensed phase.[47] The hydrogen-bond stretching frequency of the Cu−en complex increases from the free ligand (193 cm^{-1}, MP2) through the neutral molecule (197 cm^{-1}) to the ion (214 cm^{-1}). This is because the partial charges become more negative on the hydrogen-bonded nitrogen and more positive on the hydrogen-bonded hydrogen, and the increase of the charge difference enhances the hydrogen bonding. The Mulliken charges on nitrogen are calculated to be −0.43, −0.53, and −0.57 in the free ligand, the neutral molecule, and the ion, respectively; whereas the corresponding charges on hydrogen are 0.27, 0.30, and 0.33.

3.2.2. ZEKE Spectra of Cu−meen. A representative ZEKE spectrum of Cu−meen seeded in He carrier is shown in Figure 5a. Measurements with Ar carrier were not successful. In comparison to the parent diamine complex discussed above, the spectrum of the monomethyl-substituted species exhibits a number of distinctive features. First, the 0−0 transition of Cu−meen is observed at a much lower energy (36 022 cm^{-1}) than that of Cu−en (43 491 cm^{-1}). The AIE shift (7469 cm^{-1}) from Cu−en to Cu−meen is many times larger than that from Cu−NH_3 to Cu−NH_2CH_3 (974 cm^{-1}) (Table 3), a sign of the Cu−

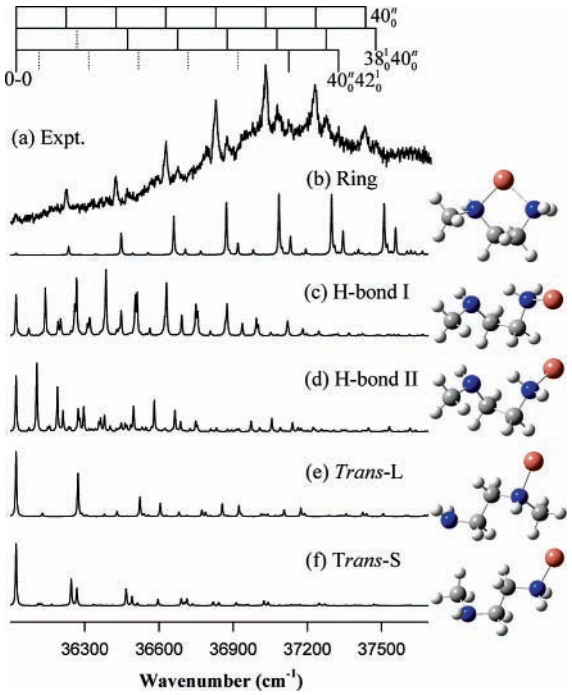

Figure 5. Experimental ZEKE spectrum of Cu−(*N*-methylethylenediamine) (a) and simulations of five Cu−(*N*-methylethylenediamine) isomers (b−f).

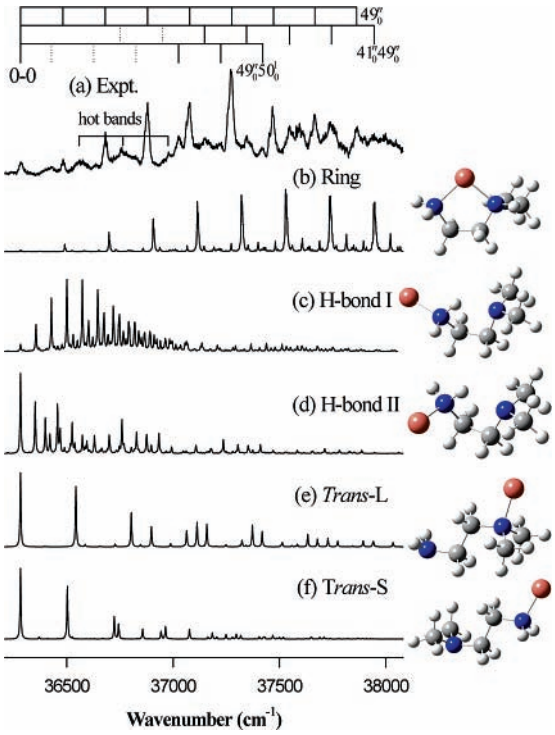

Figure 6. Experimental ZEKE spectrum of Cu−(*N*,*N*-dimethylethylenediamine) (a) and simulations of five Cu−(*N*,*N*-dimethylethylenediamine) isomers (b−f).

en and −meen complexes may have different binding modes. Second, the spectrum of Cu−meen displays a major vibrational progression (201 cm^{-1}) with a relatively long FC profile, indicating a considerable change of the geometry from the initial neutral state to the final ion state. Third, the Cu−meen spectrum displays a broader line width (16 cm^{-1}) than Cu−en and other Cu complexes investigated in our laboratory.[42,44−46] The large line width is due to unresolved rotational envelopes and perhaps unresolved sequence transitions from vibrationally hot neutral molecules as well.[48]

Figure 5b−f presents the simulations of five structural isomers of the Cu−meen complex. It is clear that only the simulation from the bidentate ring structure (Figure 5b) matches the experimental spectrum. From the experimental spectrum alone, it is not straightforward to determine whether the first peak at 36 022 cm^{-1} originates from the 0−0 transition. However, the comparison between the measured spectrum and the simulation of the ring structure suggests that this lowest-energy transition is indeed the band origin. The 201 cm^{-1} progression is assigned to the Cu$^+$−N stretch (ν_{40}^+), where Cu$^+$ is displaced from the equilibrium geometry. The long FC profile observed for this vibrational progression is consistent with a large change (>0.15 Å) in the Cu−N distance from the neutral ground electronic state (2.19/2.16 Å) to the ionic ground state (2.01/2.01 Å). Two vibrational intervals are assigned to the fundamental excitations of two NCCNC twists (248 cm^{-1} for ν_{38}^+ and 95 cm^{-1} for ν_{42}^+). These two intervals combined with the major progression 40_0^n form progressions $38_0^1 40_0^n$ and $40_0^n 42_0^1$ (Figure 5a). The signal for the first few low-energy transitions of $38_0^1 40_0^n$ and $40_0^n 42_0^1$ was too small to be observed, and their expected positions are marked with dotted lines in Figure 5a. Since the sum of the calculated ν_{38}^+ (259 cm^{-1}) and ν_{40}^+ (213 cm^{-1}) frequencies is virtually the same as that of ν_{35}^+ (471 cm^{-1}), $35_0^1 40_0^{n-1}$ transitions overlap with $38_0^1 40_0^n$. From the FC factor calculations, the relative intensity of $35_0^1 40_0^{n-1}$ versus $38_0^1 40_0^n$ is ∼20% for $n = 2$ and increased to ∼50% for $n = 5$. Therefore, the $35_0^1 40_0^{n-1}$ transitions may also contribute to the observed ZEKE spectrum. This assignment yields the experimental ν_{35}^+ frequency of 449 cm^{-1}. The ν_{35}^+ mode is identified as a Cu$^+$−N stretch, where the nitrogen atom is displaced from the equilibrium position. The assignment for each ZEKE transition is summarized in Table 4.

3.2.3. ZEKE Spectra of Cu−dmen. The dimethyl-substituted complex exhibits a similar spectral profile as the monomethyl species (Figure 6a). The spectrum begins at 36 248 cm^{-1} and extends with a long vibrational progression of 199 cm^{-1}. It shows two more progressions formed by the combination of the 199 cm^{-1} spacing with the 469 and 144 cm^{-1} intervals, respectively, and a few hot transitions. By comparing the measured spectrum with the simulations in Figure 6b−f, the Cu−dmen complex is identified to be a bidentate cyclic structure (Figure 6b). The 199 cm^{-1} progression, labeled 49_0^n in Figure 6a, is assigned to the transitions from the neutral ground state to various Cu$^+$−N stretching levels of the ion state. The Cu$^+$−N stretching motion of ν_{49}^+ is characterized by the displacement of the Cu atom and has almost the same frequency as the corresponding stretching mode of Cu$^+$−meen (ν_{40}^+, 201 cm^{-1}). The 469 cm^{-1} interval corresponds to the excitation of another Cu$^+$−N stretching with the displacement of the N atoms (ν_{41}^+) and is similar to the corresponding Cu$^+$−N stretching of Cu−en (ν_{28}^+, 474 cm^{-1}) and Cu−meen (ν_{35}^+, 449 cm^{-1}). The 144 cm^{-1} interval is identified as the excitation of a N(CH$_3$)$_2$ rocking mode (ν_{50}^+) in the ion. The three hot band transitions at 36 559, 36 764, and 36 977 cm^{-1} (Figure 6a) are assigned to $49_0^2 50_1^0$, $48_0^1 49_0^2 50_1^0$, and $48_0^2 49_0^2 50_1^0$, respectively, which yields vibrational frequencies of 209 cm^{-1} for ν_{48}^+ and 123 cm^{-1} for ν_{50}. ν_{48}^+ is a N−Cu$^+$−N bending mode in the ion, and ν_{50} is the N(CH$_3$)$_2$ rocking mode in the neutral complex. Two additional transitions at 37 596 and 37 999 cm^{-1} (Table 4) may be assigned to the excitations of a CH$_2$ rocking mode (ν_{25}^+) and a NH$_2$ scissoring mode (ν_{13}^+) in the ion, respectively. The measured CH$_2$ rocking and NH$_2$ scissoring frequencies are 1312 and 1646 cm^{-1}, in good agreement with the calculated values of 1334

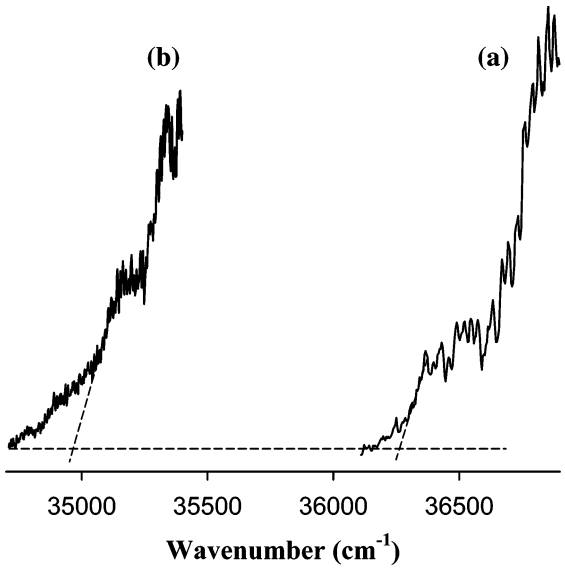

Figure 7. Photoionization efficiency spectra of Cu−(*N*,*N*,*N*′-trimethylethylenediamine) (a) and −(*N*,*N*,*N*′,*N*′-tetramethylethylenediamine) (b).

and 1644 cm^{-1}, respectively. However, because the FC factors of these two excitations are calculated to be small, their assignments are considered to be tentative.

3.2.4. Photoionization Efficiency Spectra of Cu−tren and −tmen. The ZEKE measurements on the trimethyl- and tetramethyl-substituted complexes were not successful. However, PIE measurements yielded approximate ionization energies for these two complexes. Figure 7 presents the PIE spectra of Cu−tren (a) and −tmen (b), with the Cu^+−tren signal beginning at ∼36 100 cm^{-1} and the Cu^+−tmen signal starting at ∼34 800 cm^{-1}. An extrapolation of the most steeply rising ion signal to the baseline of the spectrum gives ionization energies of 36 250-(300) cm^{-1} for Cu−tren and 34 950(300) cm^{-1} for Cu−tmen. These values have been corrected by +110 cm^{-1}, the energy shift induced by the electric field (320 V cm^{-1}) used in recording the PIE spectra. The signal below the estimated ionization threshold may be due to ionization of thermally excited molecules. There appears to be a second signal onset at ∼400 cm^{-1} (above the first onset) in the trimethyl-substituted species and ∼200 cm^{-1} in the tetramethyl derivative. The second onset may indicate the opening of the first excitation of a vibrational mode in the ion complex, but definitive assignment is difficult because of the large measurement uncertainty. The large uncertainty is due to the slowly rising ion signal as the laser is scanned to shorter wavelengths. The lack of the sharp onset at the ionization threshold may be due to a large structural change upon ionization or hot transitions from excited vibrational levels of the neutral complexes. However, since the trimethyl and tetramethyl species have similar ionization energies as the monomethyl and dimethyl derivatives, they are expected to be in the bidentate binding configuration as well. This is supported by the MP2 predictions that the bidentate cyclic isomer has the lowest energy in both the trimethyl and tetramethyl species (Table 2).

3.2.5. Comparison of Experimental Measurements and ab Initio Calculations. From the ZEKE measurements, the most stable neutral Cu−en complex is a hydrogen-bond stabilized monodentate structure and the methyl-substituted derivatives are bidentate structures. The MP2 calculations correctly predict the minimum-energy geometry (H-bond I) for Cu−en, but the theoretical predictions give the bidentate structure slightly higher energies (∼2 kJ mol^{-1}) than H-bond II monodentate structure for Cu−meen and −dmen. Table 5 summarizes the AIEs and vibrational frequencies of the observed isomers of the Cu complexes from the ZEKE spectra and MP2 calculations. Overall, the calculated frequencies for vibrational modes of larger than about 200 cm^{-1} are in good agreement with the experimental values. However, the ab initio results for lower-frequency modes are mixed, with relative errors ranging from −3% for the N−$(CH_3)_2$ rocking mode of Cu−dmen to 77% for the Cu−N−C−C torsion of Cu−en. For ionization energies, the calculated values are uniformly lower than the measured values by 3000−4000 cm^{-1} (36−48 kJ mol^{-1}). Therefore, the experimental measurements of ionization energies and low-frequency modes are especially valuable, as the theory is still not able to do a good job. More expensive methods and basis sets may be used to improve the theoretical results, but this is beyond the current work.

4. Conclusions

We report a spectroscopic and ab initio study of the copper complexes of ethylenediamine and methyl-substituted derivatives. ZEKE spectra are obtained for the Cu complexes with ethylenediamine, *N*-methylethylenediamine, and *N*,*N*-dimethylethylenediamine; and PIE spectra are measured for the Cu complexes of *N*,*N*,*N*′-trimethylethylenediamine and *N*,*N*,*N*′,*N*′-tetramethylethylenediamine. A number of low-energy structures are predicted for each of the Cu complexes by the MP2 calculation. These structures involve the bidentate Cu binding to two nitrogen atoms and the monodentate Cu binding to single nitrogen with or without an internal hydrogen bond. The parent diamine complex is identified in a structure with monodentate Cu coordination and an internal hydrogen bond. In contrast, all methyl-substituted derivatives are determined to be in a cyclic structure with bidentate Cu binding. The binding modes of these complexes result from the competition between the Cu coordination and hydrogen bonding. With unsubstituted ethylenediamine, single Cu coordination plus internal hydrogen bonding is preferred over double Cu coordination. For all the methyl derivatives, the bidentate Cu binding is more stable. However, all ionic complexes are more stable with the bidentate Cu binding.

Acknowledgment. This work was supported by the Experimental Physical Chemistry Program of the National Science Foundation and the donors of the Petroleum Research Fund of the American Chemical Society.

Supporting Information Available: A table of the vibrational frequencies of the neutral and ionic Cu complexes of en, meen, and dmen from MP2 calculations. This material is available free of charge via the Internet at http://pubs.acs.org.

References and Notes

(1) Cotton, F. A.; Wilkinson, G.; Murillo, C. A.; Bochmann, M. *Advanced Inorganic Chemistry*, 6th ed.; Wiley: New York, 1999.

(2) House, D. A. Ammonia and Amine. In *Comprehensive Coordination Chemistry*; Wilkinson, G., Gillard, T. D., McCleverty, J. A., Eds.; Pergamon: Oxford, 1987; Vol. 2, p 23.

(3) Jamet-Delcroix, S. *Acta Crystallogr., Sect. B* **1973**, *29*, 977.

(4) Marques, M. P. M.; Batista de Carvalho, L. A. E.; Tomkinson, J. *J. Phys. Chem. A* **2002**, *106*, 2473.

(5) Righini, R.; Califano, S. *Chem. Phys.* **1976**, *17*, 45.

(6) Batista de Carvalho, L. A. E.; Lourenco, L. E.; Marques, M. P. M. *J. Mol. Struct.* **1999**, *482*, 639.

(7) Radom, L.; Hariharan, P. C.; Pople, J. A.; Schleyer, P. v. R. *J. Am. Chem. Soc.* **1973**, *95*, 6531.

(8) Van Alsenoy, C.; Siam, K.; Ewbank, J. D.; Schaefer, L. *THEOCHEM* **1986**, *29*, 77.

(9) Kazerouni, M. R.; Hedberg, L.; Hedberg, K. *J. Am. Chem. Soc.* **1994**, *116*, 5279.
(10) Lee, S. J.; Mhin, B. J.; Cho, S. J.; Lee, J. Y.; Kim, K. S. *J. Phys. Chem.* **1994**, *98*, 1129.
(11) Chang, Y. P.; Su, T. M.; Li, T. W.; Chao, I. *J. Phys. Chem. A* **1997**, *101*, 6107.
(12) Kudoha, S.; Takayanagia, M.; Nakataa, M.; Ishibashib, T.; Tasumic, M. *J. Mol. Struct.* **1999**, *479*, 41.
(13) Li, S.; Fuller, J. F.; Wang, X.; Sohnlein, B. R.; Bhowmik, P.; Yang, D.-S. *J. Chem. Phys.* **2004**, *121*, 7692.
(14) Ikuta, S. *Chem. Phys.* **1986**, *108*, 441.
(15) Ikuta, S. *Chem. Phys. Lett.* **1985**, *116*, 482.
(16) Liau, Y. H.; Su, T. M. *J. Am. Chem. Soc.* **1992**, *114*, 9169.
(17) Liu, H.; Sun, J.; Yang, S. *J. Phys. Chem. A* **2003**, *107*, 5681.
(18) Alcami, M.; Luna, A.; Mo, O.; Yanez, M.; Tortajada, J.; Amekraz, B. *Chem.—Eur. J.* **2004**, *10*, 2927.
(19) Alcami, M.; Luna, A.; Mo, O.; Yanez, M.; Tortajada, J. *J. Phys. Chem. A* **2004**, *108*, 8367.
(20) Rothschopf, G. K.; Perkins, J. S.; Li, S.; Yang, D.-S. *J. Phys. Chem. A* **2000**, *104*, 8178.
(21) Proch, D.; Trickl, T. *Rev. Sci. Instrum.* **1989**, *60*, 713.
(22) Moore, C. E. *Atomic Energy Levels*; National Bureau Standards: Washington, DC, 1971.
(23) Frisch, M. J.; Trucks, G. W.; Schlegel, H. B.; Scuseria, G. E.; Robb, M. A.; Cheeseman, J. R.; Montgomery, J. A., Jr.; Vreven, T.; Kudin, K. N.; Burant, J. C.; Millam, J. M.; Iyengar, S. S.; Tomasi, J.; Barone, V.; Mennucci, B.; Cossi, M.; Scalmani, G.; Rega, N.; Petersson, G. A.; Nakatsuji, H.; Hada, M.; Ehara, M.; Toyota, K.; Fukuda, R.; Hasegawa, J.; Ishida, M.; Nakajima, T.; Honda, Y.; Kitao, O.; Nakai, H.; Klene, M.; Li, X.; Knox, J. E.; Hratchian, H. P.; Cross, J. B.; Bakken, V.; Adamo, C.; Jaramillo, J.; Gomperts, R.; Stratmann, R. E.; Yazyev, O.; Austin, A. J.; Cammi, R.; Pomelli, C.; Ochterski, J. W.; Ayala, P. Y.; Morokuma, K.; Voth, G. A.; Salvador, P.; Dannenberg, J. J.; Zakrzewski, V. G.; Dapprich, S.; Daniels, A. D.; Strain, M. C.; Farkas, O.; Malick, D. K.; Rabuck, A. D.; Raghavachari, K.; Foresman, J. B.; Ortiz, J. V.; Cui, Q.; Baboul, A. G.; Clifford, S.; Cioslowski, J.; Stefanov, B. B.; Liu, G.; Liashenko, A.; Piskorz, P.; Komaromi, I.; Martin, R. L.; Fox, D. J.; Keith, T.; Al-Laham, M. A.; Peng, C. Y.; Nanayakkara, A.; Challacombe, M.; Gill, P. M. W.; Johnson, B.; Chen, W.; Wong, M. W.; Gonzalez, C.; Pople, J. A. *Gaussian 03*, revision C.02; Gaussian, Inc.: Wallingford, CT, 2004. Frisch, M. J.; Trucks, G. W.; Schlegel, H. B.; Scuseria, G. E.; Robb, M. A.; Cheeseman, J. R.; Zakrzewski, V. G.; Montgomery, J. A., Jr.; Stratmann, R. E.; Burant, J. C.; Dapprich, S.; Millam, J. M.; Daniels, A. D.; Kudin, K. N.; Strain, M. C.; Farkas, O.; Tomasi, J.; Barone, V.; Cossi, M.; Cammi, R.; Mennucci, B.; Pomelli, C.; Adamo, C.; Clifford, S.; Ochterski, J.; Petersson, G. A.; Ayala, P. Y.; Cui, Q.; Morokuma, K.; Malick, D. K.; Rabuck, A. D.; Raghavachari, K.; Foresman, J. B.; Cioslowski, J.; Ortiz, J. V.; Stefanov, B. B.; Liu, G.; Liashenko, A.; Piskorz, P.; Komaromi, I.; Gomperts, R.; Martin, R. L.; Fox, D. J.; Keith, T.; Al-Laham, M. A.; Peng, C. Y.; Nanayakkara, A.; Gonzalez, C.; Challacombe, M.; Gill, P. M. W.; Johnson, B. G.; Chen, W.; Wong, M. W.; Andres, J. L.; Head-Gordon, M.; Replogle, E. S.; Pople, J. A. *Gaussian 98*, revision A.11; Gaussian, Inc.: Pittsburgh, PA, 1998.
(24) Yang, D.-S.; Zgierski, M. Z.; Rayner, D. M.; Hackett, P. A.; Martinez, A.; Salahub, D. R.; Roy, P.-N.; Carrington, T., Jr. *J. Chem. Phys.* **1995**, *103*, 5335.
(25) Berces, A.; Zgierski, M. Z.; Yang, D.-S. *Computational Molecular Spectroscopy*; Wiley: New York, 2000.
(26) Duschinsky, F. *Acta Physicochim. URSS* **1937**, *7*, 551.
(27) Bondi, A. *J. Phys. Chem.* **1964**, *68*, 441.
(28) Boses, A. D.; Chandra, A.; Martin, J. M. L.; Marx, D. *J. Chem. Phys.* **2003**, *119*, 5965.
(29) Perez, P.; Simon-Manso, Y.; Aizman, A.; Fuentealba, P.; Contreras, R. *J. Am. Chem. Soc.* **2000**, *122*, 4756.
(30) Lakard, B.; Herlem, G.; Fahys, B. *THEOCHEM* **2002**, *584*, 15.
(31) Maksic, Z. B.; Vianello, R. *J. Phys. Chem. A* **2002**, *106*, 419.
(32) Allen, L. C. *J. Am. Chem. Soc.* **1975**, *97*, 6921.
(33) Del Bene, J. E. *J. Chem. Phys.* **1972**, *57*, 1899.
(34) Kollman, P. A.; Allen, L. C. *Chem. Rev.* **1972**, *72*, 283.
(35) Calhorda, M. J. *Chem. Commun.* **2000**, 801.
(36) Cotton, F. A.; Daniels, L. M.; Jordan, G. T. I. V.; Murillo, C. A. *Chem. Commun.* **1997**, 1673.
(37) Desiraju, G. R. *Chem. Commun.* **2005**, 2995.
(38) Mascal, M. *Chem. Commun.* **1998**, 303.
(39) Rothschopf, G. K.; Li, S.; Shannon Perkins, J.; Yang, D.-S. *J. Chem. Phys.* **2001**, *115*, 4565.
(40) Li, S.; Fuller, J. F.; Sohnlein, B. R.; Yang, D.-S. *J. Chem. Phys.* **2003**, *119*, 8882.
(41) Li, S.; Rothschopf, G. K.; Fuller, J. F.; Yang, D.-S. *J. Chem. Phys.* **2003**, *118*, 8636.
(42) Miyawaki, J.; Sugawara, K.; Li, S.; Yang, D.-S. *J. Phys. Chem. A* **2005**, *109*, 6697.
(43) Wang, X.; Yang, D.-S. *J. Phys. Chem. A* **2004**, *108*, 6449.
(44) Li, S.; Sohnlein, B. R.; Rothschopf, G. K.; Fuller, J. F.; Yang, D.-S. *J. Chem. Phys.* **2003**, *119*, 5406.
(45) Miyawaki, J.; Sugawara, K. *J. Chem. Phys.* **2003**, *119*, 6539.
(46) Li, S.; Sohnlein, B. R.; Yang, D.-S.; Miyawaki, J.; Sugawara, K.-I. *J. Chem. Phys.* **2005**, *122*, 214316/1.
(47) Bennett, A., M. A.; Foulds, G. A.; Thornton, D. A. *Spectrochim. Acta* **1989**, *45A*, 219.
(48) Fuller, J. F.; Li, S.; Sohnlein, B. R.; Rothschopf, G. K.; Yang, D.-S. *Chem. Phys. Lett.* **2002**, *366*, 141.